Evaluation of an hybrid POD formulation for responses under prescribed displacements

Antoine Placzek, Duc-Minh Tran, Roger Ohayon

Evaluation of an Hybrid POD Formulation for Responses under Prescribed Displacements

A. Placzek[1,2]**, D.-M. Tran**[1]**, R. Ohayon**[2]

[1] Onera, The French Aerospace Lab,
Aeroelasticity & Structural Dynamics Dpt.,
29, avenue de la Division Leclerc,
BP 72, 92320 Châtillon, France
e-mail: **antoine.placzek@onera.fr**

[2] Conservatoire National des Arts et Métiers (CNAM)
Structural Mechanics & Coupled Systems Laboratory
2, rue Conté
75003 Paris, France

Abstract

Hybrid Proper Orthogonal Decomposition formulation is a POD based reduced-order modeling method where the continuous equation of the physical system is projected on the POD modes obtained from a discrete model of the system. The hybrid POD formulation is evaluated here on the simple case of a linear elastic rod subject to a prescribed displacement imposed at the free end of the rod. Three techniques are used and compared to take into account the non-homogeneous boundary condition with the hybrid POD: the first method relies on Control Functions, the second on the Penalty Method and the third on Lagrange Multipliers. Finally the robustness of the hybrid POD is investigated.

1 Introduction

The Proper Orthogonal Decomposition (POD) is a powerful method providing the description of a high-dimensional system by means of a small number of elements, called the POD modes (POMs). These POMs contain the main characteristics of the system response such that the solution of the system can be reconstructed as a linear combination of the POMs. The method is closely related to the Karhunen-Loève decomposition originating from the probability theory [1] and to the Principal Component Analysis commonly used in the field of statistics. Connexions with the Singular Value Decomposition can also be highlighted [2] and Liang et al. [3] demonstrated the equivalence between the three preceding methods when they are used to handle discrete random vectors of finite dimension.

The starting point of the POD is a set of snapshots describing the system and obtained either from numerical simulations or experiments. The set of snapshots is combined into a correlation tensor, whose properties ensure that real eigenvectors exist. These eigenvectors are the POD modes and represent the coherent structures of the system. The most important feature of the POD is its optimality: for a given number of POMs, the POD basis containing these modes provides the best approximation of any element of the snapshots set. The POD is therefore a powerful technique for data analysis since an important database can be efficiently represented by only a small number of modes.

However the method is not restricted to data analysis but can be combined with the equation governing a dynamical system to form a reduced order model. The POD has therefore been extensively used for fluid dynamics systems since the early work of Lumley [4] as it provides an efficient mean to build a reduced-order model. Unlike the eigenmode reduction technique commonly used in structural dynamics, the POD has two main advantages : (i) it can as well be formulated for a linear or a non-linear system and (ii) the POMs can be obtained from the resolution of an eigenproblem whose dimension is equal to the number of snapshots and is consequently very small compared to the number of degrees of freedom. The construction of POD reduced-order models for the fluid has therefore expanded rapidly since the first works and a great part of

the POD literature is devoted to fluid reduced-order models that could be built for a wide variety of flows to perform parametric studies or active control. Since the present paper focuses on a structural test case, the construction of POD reduced-order models for the fluid is not detailed here but the reader is referred to review articles like those of Lucia et al. [5] or Dowell et al. [6] for more details.

Historically, the POD-Galerkin method has been introduced for fluid dynamics systems but the technique has spread over various mechanical systems and notably structural mechanics ones. Kerschen et al. [7] give an overview of the general method and several examples of the use of POD. The POD method provides an interesting alternative to the classical eigenmode reduction and is especially useful for non-linear systems. Indeed, Feeny and Kappagantu [8] and Kerschen and Golinval [9] explained that the POMs converge to the eigenmodes of an undamped and unforced linear system when the mass matrix is proportional to identity and if a sufficient number of snapshots is considered. The POD is thus preferably applied to non-linear systems [10, 11], sometimes subject to vibro-impacts [12]. However, Sampaio and Soize [13] claim that the POD basis is not more efficient than the eigenmodes basis for non-linear elastodynamics.

The construction of reduced-order models can be handled in different ways according to the nature (discrete or continuous) of the equation and snapshots used and the formulation often differs when fluids or solids are considered. For structural dynamics problems, the discrete equation of the system is generally available (for example by means of the mass, damping and stiffness matrices) and the reduced-order model can be easily obtained by projecting the discrete operators on the discrete POMs, hence the name of *discrete POD* for this approach. However the discretized equation is not always explicitly known: this is the case for example if we want to model a non-linear fluid flow, or if we work with experimental data. In this case, we only know the continuous equation of the system but we have discrete POMs (coming from numerical simulations or sensors). This leads to an *hybrid POD* since the discrete POMs are used in conjunction with the continuous equation. The reduced-order model is then built by projecting the continuous equations on each POM according to the Galerkin method. These two formulations of the POD method have been compared by Placzek et al. [14] to a third formulation based on an analytical solution and the hybrid POD method proved to be slightly more efficient than the discrete POD formulation.

Since our aim is to build later reduced-order models for fluid-structure systems, we focus on the hybrid POD which is the common approach adopted for fluids. When dealing with fluid-structure interaction problems, the coupling condition between the fluid and the structure involves prescribed displacements on the fluid-structure interface. It is therefore of prime importance to investigate the forced response with prescribed displacements (non-homogeneous boundary condition) in the hybrid POD reduced-order model. Homogeneous boundary conditions are easily taken into account since those properties are inherited by the POMs. However, when non-homogeneous boundary conditions are applied to the system, the POD reduced-order model has to be adapted so that the boundary condition is satisfied. Three techniques are considered here to take into account a displacement imposed at the free end. The first method relies on a weak formulation of the boundary condition: the strong non-homogeneous Dirichlet boundary condition is transformed into a weak Neumann boundary condition by means of a small parameter whose inverse will be called the penalty factor. This method is therefore called the Penalty Method (PM). In the second approach, the system can be considered as a problem with a constraint which, in this case, represents the boundary condition that must be verified. The constraint is treated by means of a Lagrange multiplier, hence the name of Lagrange Multiplier Method (LMM) for the formulation. The last technique is based on a different formulation of the POD in which the POMs are computed from snapshots that have been previously homogenized. The homogenization step uses a suitably chosen "Control Function" that can be changed later in the reduced-order model to have the desired boundary condition. According to the paper of Tang et al. [15], this formulation will be called the Control Function Method (CFM).

The paper is organized as follows: the principle of the POD method and the construction of the hybrid POD reduced-order model are presented in section 2. Then the different techniques (CFM, PM and LMM) developed to take into account the non-homogeneous boundary condition for the forced response are presented and evaluated in section 3. Finally, in section 4, the robustness of the hybrid POD is investigated.

2 The hybrid POD formulation

2.1 The Proper Orthogonal Decomposition (POD) method

The POD method is presented here in the context of a deterministic system and we do not refer to the Karhunen-Loève theorem usually adduced in the stochastic setting. The description, close to the one of Holmes et al. [16], relies on an optimization problem which consists in finding the best basis to approximate a set of snapshots. The snapshots are in fact solutions $u^{(k)}$ of the system evaluated at different instants t_k and the snapshots set $U = \left\{u^{(k)} \in H, k = 1, .., M\right\}$ gathers a finite number of them . The solutions are contained in a Hilbert space H with $N = \dim(H)$ (N being eventually infinite), whose vectors can be continuous squared integrable functions on a spatial domain Ω ($H = L^2(\Omega)$) or real discrete finite vectors ($H = \mathbb{R}^N$) for example. Let $\langle \cdot, \cdot \rangle$ be the inner product associated to the Hilbert space H and $\|\cdot\|$ denote the norm induced by this inner product so that $\forall x \in H, \|x\|^2 = \langle x, x \rangle$.

The POD consists then in finding a subspace $S \subset H$ of finite dimension $q \ll N$ which provides the best approximation of any member of U. This subspace is entirely characterized by the basis $\left\{\varphi^{(j)} \in H, j = 1, .., q\right\}$ so that $S = \text{span}\left\{\varphi^{(1)}, ..., \varphi^{(q)}\right\}$. Each snapshot can therefore be approximated on the subspace S by a linear combination of the POMs $\varphi^{(j)}$:

$$u^{(k)} = \sum_{j=1}^{q} a_j^{(k)} \varphi^{(j)} \qquad \forall k \in [1; M], \tag{1}$$

where the $a_j^{(k)}$ are real scalars representing the modal amplitudes associated to the mode $\varphi^{(j)}$ in the decomposition of the snapshot $u^{(k)}$. The subspace S has to be sought so that the basis $\left\{\varphi^{(j)}\right\}_{j=1}^{q}$ is optimal in the sense that it is better than any other basis of same dimension q. To ensure optimality, we impose that the time-averaged squared projection error $E\left(\left\|u^{(k)} - \mathcal{P}_S\, u^{(k)}\right\|^2\right)$ is minimal. The time-averaging operation for a function $f\left(u^{(k)}\right)$ depending on the snapshots is the sum $E\left(f\left(u^{(k)}\right)\right) = \sum_{k=1}^{M} \alpha_k f\left(u^{(k)}\right)$ where the α_k are weighting coefficients. The minimization problem is equivalent to maximizing the time-averaged squared projection of the snapshots $E\left(\left\|\mathcal{P}_S\, u^{(k)}\right\|^2\right)$. Indeed the operator $\mathcal{P}_S$ defines an orthogonal projection on the subspace S in order to minimize the distance between each snapshot in H and its approximation in S. Developing the expression of the orthogonal projector in $\mathcal{P}_S u^{(k)} = \sum_{j=1}^{q} \left\langle u^{(k)}, \varphi^{(j)} \right\rangle \varphi^{(j)}$ and using the orthonormality of the POMs, the mathematical statement of optimality is to find the

$$\max_{\varphi^{(j)} \in H, \left\|\varphi^{(j)}\right\| = 1} \quad \sum_{j=1}^{q} E\left(\left\langle u^{(k)}, \varphi^{(j)} \right\rangle^2\right) \tag{2}$$

for suitably normalized POMs $\varphi^{(j)}$. The problem of finding the maximum subject to the constraint $\left\|\varphi^{(j)}\right\| = 1$ can be transformed into the following variational problem defined for the functional J:

$$J\left[\varphi^{(j)}\right] = E\left(\left\langle u^{(k)}, \varphi^{(j)} \right\rangle^2\right) - \lambda_j \left(\left\|\varphi^{(j)}\right\|^2 - 1\right) \tag{3}$$

A necessary condition to obtain the maximum is that the functional derivative vanishes for all variations $\varphi^{(j)} + \delta\psi \in H, \delta \in \mathbb{R}$. After some mathematical manipulations (for more details, see Holmes et al. [16]), the preceding condition which must be true for all variation ψ, turns out to be equivalent to solving the following eigenvalue problem:

$$R\,\varphi^{(j)} = \lambda_j\, \varphi^{(j)} \qquad \forall j \in [1; q] \tag{4}$$

where the operator R is an endomorphism of H defined by:

$$R = E\left(u^{(k)} \otimes (u^{(k)})^*\right) \tag{5}$$

In the preceding expression, $(u^{(k)})^*$ is the dual of the vector $u^{(k)}$, i.e. the linear application defined by $(u^{(k)})^* : v \longrightarrow (u^{(k)})^* v = \left\langle v, u^{(k)} \right\rangle, \forall v \in H$ and $\otimes$ is the usual tensor product so that $w \otimes (u^{(k)})^* v = w \left\langle v, u^{(k)} \right\rangle, \forall v, w \in H$. The operator R is self-adjoint and has a finite rank r since it is spanned by the snapshots. R is therefore a Hilbert-Schmidt operator and is consequently compact. With these properties the spectral theory for compact self-adjoint operators is valid and ensures that there is only a finite number r of real non-null eigenvalues λ_j. The associated eigenvectors which are the POMs we looked for are orthonormal.

Taking the inner product of Eq. (4) with $\varphi^{(j)}$ and using the expression Eq. (5) of the operator R lead to the following relation:

$$\lambda_j = E\left(\left\langle u^{(k)}, \varphi^{(j)} \right\rangle^2\right) \tag{6}$$

The preceding relation indicates that the greatest eigenvalues λ_j maximize in average the projection of the snapshots on the POMs. Consequently the greatest eigenvalues capture the most of "energy" contained in the snapshots set in the sense of the norm induced by the Hilbert space. In order to be efficient, the reduced-order model constructed with the POMs has therefore to be composed of the first $q \leq r$ eigenvectors associated to the largest eigenvalues.

The extraction of the POMs becomes very laborious when the size of the problem becomes important as the dimension of the operator R is related to the number N of degrees of freedom in the system. A powerful variant called the snapshots method proposed by Sirovich [17] reduces considerably the size of the problem to be solved. The method is based on the fact that the POMs are a linear combination of the snapshots:

$$\varphi^{(j)} = \sum_{k=1}^{M} c_k^{(j)} u^{(k)} \tag{7}$$

since the image of R is a subset of the space spanned by the snapshots. Introducing Eq. (7) into Eq. (4) with the expression Eq. (5) of R leads, after reorganization of the terms, to:

$$\sum_{k=1}^{M} \left(\sum_{l=1}^{M} \alpha_k \left\langle u^{(k)}, u^{(l)} \right\rangle c_l^{(j)} \right) u^{(k)} = \lambda_j \sum_{m=1}^{M} c_m^{(j)} u^{(m)} \tag{8}$$

If the snapshots are assumed to be linearly independent, the previous expression reduces to the new eigenvalue problem whose dimension is now $M \ll N$:

$$\sum_{l=1}^{M} \alpha_k \left\langle u^{(k)}, u^{(l)} \right\rangle c_l^{(j)} = \lambda_j c_k^{(j)} \qquad \forall k \in [1; M] \tag{9}$$

The previous relation can be transposed in the matricial form $\widetilde{\mathbf{R}}^* \mathbf{c}^{(j)} = \lambda_j \mathbf{c}^{(j)}$ with $\widetilde{R}^*_{ij} = \alpha_i \left\langle u^{(i)}, u^{(j)} \right\rangle$ and $\mathbf{c}^{(j)} = [c_1^{(j)} \cdots c_M^{(j)}]^T$. However the matrix $\widetilde{\mathbf{R}}^*$ is not symmetrical except if all the weights α_i associated to the time-averaging operator $E(\cdot)$ are identical. If all weights are strictly positive, the problem can be symmetrized by using the matrix $\widetilde{\boldsymbol{\alpha}} = \text{diag}(\sqrt{\alpha_1}, \ldots, \sqrt{\alpha_M})$. The eigenvalue problem obtained with the snapshots method is finally:

$$\mathbf{R}^* \mathbf{d}^{(j)} = \lambda_j \mathbf{d}^{(j)} \tag{10}$$

where $R^*_{ij} = \sqrt{\alpha_i \alpha_j} \left\langle u^{(i)}, u^{(j)} \right\rangle$ and the eigenvectors are related to the coefficients $\mathbf{c}^{(j)}$ of the decomposition Eq. (7) by the following relation $\mathbf{c}^{(j)} = \widetilde{\boldsymbol{\alpha}} \mathbf{d}^{(j)}$.

The snapshots method has been obtained here for snapshots of possibly infinite dimension. The equivalence with the direct method holds only if the snapshots are linearly independent, so that one can infer Eq. (9) from Eq. (8). If snapshots of finite dimension are considered, it is not necessary to assume that they are linearly independent. The equivalence between the direct method and the snapshots method can be proved for example by using the Singular Value Decomposition of the matrix containing the snapshots of finite dimension. In this case, the snapshots method provides as many POMs as the rank r of the snapshots matrix and the POMs are strictly identical to those of the direct method. For practical applications, finite dimension snapshots are always used and consequently the snapshots method will be preferably adopted in the remainder of this paper.

It should also be noted that better results are obtained when the POD is performed for the fluctuations $s^{(k)}$ of the data rather than for the raw data $u^{(k)}$. Indeed, Tamura et al. [18] observed that if the POD is carried out directly for the snapshots $u^{(k)}$, the first POD mode is rather similar to the mean of the snapshots and the eigenspectra is distorted. The fluctuations, or centered data, are defined by $s^{(k)} = u^{(k)} - \overline{u}$, where $\overline{u} = E\left(u^{(k)}\right)$ represents the time-average of the snapshots. The operators R and R^* are thus based on the $s^{(k)}$ instead of the $u^{(k)}$ and the decomposition Eq. (1) of the snapshots is modified in:

$$u^{(k)} = \overline{u} + \sum_{j=1}^{q} a_j^{(k)} \varphi^{(j)} \qquad \forall k \in [1; M] \tag{11}$$

2.2 Construction of a reduced-order model with the hybrid POD formulation

Now that we have described in the previous paragraph how the POMs associated to a system can be obtained from a set of snapshots, we turn to the construction of a reduced-order model which uses these POMs in the context of an hybrid POD formulation. The reduced-order model is built for a one dimensional rod subject to traction and compression which is characterized by its length L, the section S and the material is represented by the Young's modulus E and the density ρ. In absence of external forces, the displacement $u(x,t)$ of the rod section at a given point x and at time t is governed by the wave equation:

$$\rho S \frac{\partial^2 u}{\partial t^2} - ES \frac{\partial^2 u}{\partial x^2} = 0 \tag{12}$$

The aim of the hybrid POD formulation is to use a discrete snapshots database in conjunction with the continuous equation Eq. (12) of the system. Indeed, the snapshots are almost always described by a discrete quantity coming either from a numerical simulation or an experiment but the discrete equation that could be combined with this discrete approximation of the snapshots is not always available. The discrete dataset available is thus used to approximate directly the L^2 inner product which appears in the hybrid POD formulation since it relies on the continuous equation of the system. The inner product of two continuous functions f and g is therefore approximated by the trapezoidal rule:

$$\langle f, g \rangle_{L^2(\Omega)} = \int_\Omega f(x)\, g(x)\, d\Omega = \sum_{e=1}^{N} \int_{\Omega_e} f(x)\, g(x)\, d\Omega \approx \sum_{e=1}^{N} \widehat{f}_e\, \widehat{g}_e\, \delta\Omega_e \tag{13}$$

where $\widehat{f}_e$ and $\widehat{g}_e$ are the average values relative to the functions f and g evaluated on each element e and $\delta\Omega_e$ is the Lebesgue measure of the element Ω_e. The previous expression takes the matricial form:

$\langle f, g \rangle_{L^2(\Omega)} \approx \widehat{\mathbf{f}}^T \, \boldsymbol{\Delta} \, \widehat{\mathbf{g}}$ with $\widehat{\mathbf{f}} = [\widehat{f}_1 \cdots \widehat{f}_N]^T$ (resp. for $\widehat{\mathbf{g}}$) and $\boldsymbol{\Delta} = \text{diag}(\delta\Omega_1, \cdots, \delta\Omega_N)$. As the problem is unidimensional, the average values of the function f on one element is simply given here by the arithmetic mean $\widehat{f}_i = (f_i + f_{i+1})/2$, where the f_i are the values contained in the dataset and which are supposed to be the values at the nodes of the mesh.

The correlation tensor $\mathbf{R}^*$ is defined by the L^2 inner product since the reduced-order model is built from the continuous equation. The inner product is then approximated with Eq. (13) so that the general term of $\mathbf{R}^*$ is: $R^*_{ij} = \sqrt{\alpha_i \alpha_j} \left\langle s^{(i)}, s^{(j)} \right\rangle_{L^2} \approx \sqrt{\alpha_i \alpha_j} \left(\widehat{\mathbf{s}}^{(i)} \right)^T \boldsymbol{\Delta} \, \widehat{\mathbf{s}}^{(j)}$. With matricial notations, the previous relation is rewritten as $\mathbf{R}^* = \left(\widetilde{\boldsymbol{\alpha}}^T \, \widehat{\mathbf{S}}^T \right) \boldsymbol{\Delta} \left(\widehat{\mathbf{S}} \, \widetilde{\boldsymbol{\alpha}} \right)$. The POMs extracted from the eigenvalue problem are discrete like the snapshots they have been derived from. In order to build the reduced-order model, the continuous POD decomposition Eq. (11) is substituted into the governing equation (12) and the resulting expression is projected onto each POM $\varphi^{(j)}$. Using the orthonormality of the POMs and denoting $c = \sqrt{E/\rho}$, the equation writes :

$$\frac{d^2 a_j}{dt^2} = c^2 \sum_{k=1}^{q} \left\langle \frac{d^2 \varphi^{(k)}}{dx^2}, \varphi^{(j)} \right\rangle a_k + c^2 \left\langle \frac{d^2 \overline{u}}{dx^2}, \varphi^{(j)} \right\rangle \tag{14}$$

The q equations obtained by projecting on each POM can be gathered in the matricial ordinary differential equation $\ddot{\mathbf{a}} = \breve{\boldsymbol{\mathcal{L}}} \mathbf{a} + \breve{\boldsymbol{\mathcal{K}}}$ defining the unknown amplitudes $\mathbf{a} = [a_1 \ldots a_q]^T$ of the decomposition Eq. (11). The computation of the coefficients $\breve{\mathcal{L}}_{kj} = c^2 \left\langle d^2 \varphi^{(k)}/dx^2, \varphi^{(j)} \right\rangle$ and $\breve{\mathcal{K}}_j = c^2 \left\langle d^2 \overline{u}/dx^2, \varphi^{(j)} \right\rangle$ of the reduced-order model requires that the derivatives of the POMs are known. The derivatives can be computed for example by means of Finite Difference Methods. It should also be mentioned that the inner products can be simplified by performing parts integrations which introduce the boundary conditions in the expression of the coefficients. In the case of the free response to an initial condition for example, the order of the derivatives can be lowered and the integrals on the boundary vanish since the boundary conditions are homogeneous (see Placzek et al. [14] for more details).

3 Hybrid POD formulations for the response to a prescribed displacement

In the case of a clamped rod with a prescribed displacement $\gamma(t)$ imposed at the free end, the boundary conditions are:

$$\begin{cases} u(x = 0, t) = 0 \\ u(x = L, t) = \gamma(t) \end{cases} \qquad \forall t > 0 \tag{15}$$

The Dirichlet boundary condition at the free-end is non-homogeneous and consequently the POMs do not inherit this property: this boundary condition is not implicitly satisfied by the reduced-order model through the POMs and it must be explicitly imposed. Several techniques are presented in the following for the hybrid POD formulation to take into account this non-homogeneous boundary condition.

3.1 The Penalty Method (PM)

The Penalty Method is often used to impose Dirichlet boundary conditions in structural problems and has already been used by Tang et al. [15] in the context of POD reduced-order model. The principle consists in replacing the strong Dirichlet boundary condition $u(x = L, t) = \gamma(t)$ by the artificial Neumann boundary condition:

$$\left.\frac{\partial u}{\partial x}\right|_{x=L} = \frac{u_L - \gamma(t)}{\varepsilon} \tag{16}$$

where ε is a parameter small enough to satisfy approximately the boundary condition with $u_L = u(x = L, t)$. We define the penalty factor $f_p = c^2/\varepsilon$ whose value has to be great so as to $u_L = \gamma(t)$ when $f_p \to \infty$. The artificial Neumann boundary condition can be explicitly introduced in the reduced-order model by performing one parts integration in the inner products of Eq. (14). The boundary term corresponding to the homogeneous boundary condition at the clamped side is equal to zero since the POMs inherit the homogeneous Dirichlet boundary condition. However the boundary term where the displacement is imposed does not vanish. After reorganization of the terms, the reduced-order model becomes:

$$\begin{aligned} \rho S \frac{d^2 a_j}{dt^2} &= -ES \sum_{k=1}^{q} \left\langle \frac{d\varphi^{(k)}}{dx}, \frac{d\varphi^{(j)}}{dx} \right\rangle a_k - ES \left\langle \frac{d\overline{u}}{dx}, \frac{d\varphi^{(j)}}{dx} \right\rangle \\ &\quad + ES \left(\sum_{k=1}^{q} \left.\frac{d\varphi^{(k)}}{dx}\right|_{x=L} a_k + \left.\frac{d\overline{u}}{dx}\right|_{x=L} \right) \varphi^{(j)}(x = L) \end{aligned} \tag{17}$$

The term in brackets is in fact the spatial derivative of the variable u evaluated in $x = L$ when u is decomposed by the POD with Eq. (11). The artificial boundary condition Eq. (16) can then be replaced in Eq. (17):

$$\begin{aligned} \frac{d^2 a_j}{dt^2} &= -c^2 \sum_{k=1}^{q} \left\langle \frac{d\varphi^{(k)}}{dx}, \frac{d\varphi^{(j)}}{dx} \right\rangle a_k - c^2 \left\langle \frac{d\overline{u}}{dx}, \frac{d\varphi^{(j)}}{dx} \right\rangle \\ &\quad + f_p \left(u_L(t) - \gamma(t) \right) \varphi^{(j)}(x = L) \end{aligned} \tag{18}$$

The displacement u_L is decomposed on the POD basis with Eq. (11): $u_L = \overline{u_L} + \sum_{k=1}^{q} a_k(t) \varphi^{(k)}(x = L)$. The vector $\boldsymbol{\varphi}_L = [\varphi^{(1)}(x = L) \cdots \varphi^{(q)}(x = L)]^T$ is introduced so that the sum can be interpreted as the vector product $\boldsymbol{\varphi}_L^T \mathbf{a}$ where $\mathbf{a}$ is the vector of the modal amplitudes. The set of equations Eqs. (18) can be grouped in only one matricial equation $\ddot{\mathbf{a}} = \widetilde{\boldsymbol{\mathcal{L}}}\, \mathbf{a} + \widetilde{\boldsymbol{\mathcal{K}}}$ such that :

$$\begin{aligned} \widetilde{\boldsymbol{\mathcal{L}}} &= \boldsymbol{\mathcal{L}} + \boldsymbol{\mathcal{L}}_p \quad \text{with} \quad \boldsymbol{\mathcal{L}}_p = f_p \left(\boldsymbol{\varphi}_L \, \boldsymbol{\varphi}_L^T \right) \\ \widetilde{\boldsymbol{\mathcal{K}}} &= \boldsymbol{\mathcal{K}} + \boldsymbol{\mathcal{K}}_p \quad \text{with} \quad \boldsymbol{\mathcal{K}}_p = f_p \left(\overline{u_L} - \gamma(t) \right) \boldsymbol{\varphi}_L \end{aligned} \tag{19}$$

where the matrix $\boldsymbol{\mathcal{L}}$ and the vector $\boldsymbol{\mathcal{K}}$ are exactly the same as those which would be found for the free response with the hybrid formulation. The coefficients are given by $\mathcal{L}_{jk} = -c^2 \left\langle d\varphi^{(k)}/dx, d\varphi^{(j)}/dx \right\rangle$ and $\mathcal{K}_j = -c^2 \left\langle d\overline{u}/dx, d\varphi^{(j)}/dx \right\rangle$. The remaining terms can be considered as penalty terms whose action is to enforce the boundary condition.

3.2 The Lagrange Multiplier Method (LMM)

In this case, the displacement imposed at the free end is treated as a constraint which has to be added to the equation governing the rod. The displacement generates an unknown reaction R_γ that should be introduced in the second member of Eq. (12). This reaction R_γ is an additional unknown reflecting the constraint of the imposed displacement and is thus the Lagrange multiplier of the following problem:

$$\left\{ \begin{aligned} \rho S \frac{\partial^2 u}{\partial t^2} - ES \frac{\partial^2 u}{\partial x^2} &= R_\gamma \\ u(x = L, t) &= \gamma(t) \end{aligned} \right. \tag{20}$$

The first equation is, like before, projected onto each POM after having substituted u by its decomposition Eq. (11) on the POD basis. In the second equation, the variable u is also replaced with the same decomposition evaluated in $x = L$:

$$\left\{ \begin{array}{rcl} \rho S \dfrac{d^2 a_j}{dt^2} & = & ES \displaystyle\sum_{k=1}^{q} \left\langle \frac{d^2 \varphi^{(k)}}{dx^2}, \varphi^{(j)} \right\rangle a_k + ES \left\langle \frac{d^2 \overline{u}}{dx^2}, \varphi^{(j)} \right\rangle + \left\langle R_\gamma, \varphi^{(j)} \right\rangle \\ u(x=L,t) & = & \overline{u_L} + \displaystyle\sum_{k=1}^{q} a_k(t) \varphi^{(k)}(x=L) = \gamma(t) \end{array} \right. \tag{21}$$

Since the reaction R_γ acts in fact only at the free end, it can be defined by a Dirac distribution: $R_\gamma = r_L\, \delta(x-L)$, where the scalar r_L represents the intensity of the reaction at $x = L$. Consequently the inner product involving the reaction R_γ is simplified in: $\left\langle R_\gamma, \varphi^{(j)} \right\rangle = \int_0^L r_L\, \delta(x-L)\, \varphi^{(j)}(x)\, dx = r_L\, \varphi^{(j)}(x = L)$. The vector of the reaction projected on each POM is given by $r_L\, \boldsymbol{\varphi}_L$, where $\boldsymbol{\varphi}_L$ is the vector defined in the previous paragraph and containing the values of the POMs at the free end. This vector is also used to rewrite the second line in Eq. (21) in $\overline{u_L} + \boldsymbol{\varphi}_L^T \mathbf{a} = \gamma(t)$. The reduced-order model becomes:

$$\left\{ \begin{array}{l} \ddot{\mathbf{a}} = \breve{\boldsymbol{\mathcal{L}}}\, \mathbf{a} + \breve{\boldsymbol{\mathcal{K}}} + r_L\, \boldsymbol{\varphi}_L \\ 0 = \boldsymbol{\varphi}_L^T \mathbf{a} + \overline{u}_L - \gamma(t) \end{array} \right.$$

where the general term of the matrix $\breve{\boldsymbol{\mathcal{L}}}$ and the vector $\breve{\boldsymbol{\mathcal{K}}}$ are those found in Eq. (14). Finally the reduced-order model is formulated for the augmented variable vector $\widetilde{\mathbf{a}} = [\mathbf{a}\ r_L]^T$ and takes the new form $\widetilde{\boldsymbol{\mathcal{I}}}\, \ddot{\widetilde{\mathbf{a}}} = \widetilde{\boldsymbol{\mathcal{L}}}\, \widetilde{\mathbf{a}} + \widetilde{\boldsymbol{\mathcal{K}}}$. The detailed expression of the reduced-order model is the following, where $\mathbf{I}$ is the $q \times q$ identity matrix:

$$\begin{bmatrix} \mathbf{I} & \mathbf{0} \\ \mathbf{0} & 0 \end{bmatrix} \begin{bmatrix} \ddot{\mathbf{a}} \\ \ddot{r}_L \end{bmatrix} = \begin{bmatrix} \breve{\boldsymbol{\mathcal{L}}} & \boldsymbol{\varphi}_L \\ \boldsymbol{\varphi}_L^T & 0 \end{bmatrix} \begin{bmatrix} \mathbf{a} \\ r_L \end{bmatrix} + \begin{bmatrix} \breve{\boldsymbol{\mathcal{K}}} \\ \overline{u_L} - \gamma(t) \end{bmatrix} \tag{22}$$

3.3 The Control Function Method (CFM)

The last technique presented in this paper to take into account the non-homogeneous boundary condition is the Control Function Method commonly used to build reduced-order models for active control in flow dynamics, see [15] for example. The variable u is divided into two parts, the first verifying homogeneous boundary conditions and denoted u_h and the second representing the effects of the forcing term and denoted u_f, such that $u = u_h + u_f$ with $u_h(x = L, t) = 0$ and $u_f(x = L, t) = \gamma(t)$.

The POMs are computed for the centered *homogeneous* snapshots $s_h^{(k)} = u_h^{(k)} - \overline{u_h}$ and the POD decomposition is thus $u_h(x,t) = \overline{u_h}(x) + \sum_{k=1}^{q} a_k(t)\, \varphi_h^{(k)}(x)$. The notation $\varphi_h^{(k)}$ is now used to highlight the homogeneous character of the POMs derived from the snapshots that have been homogenized. The previous decomposition of u_h can be replaced in the relation $u = u_h + u_f$ to obtain the POD decomposition of the inhomogeneous variable u. Before doing this, it is interesting to write the forcing term u_f as the product of a spatial and a temporal function which corresponds to the temporal modulation of the boundary condition Eq. (15): $u_f(x,t) = \gamma(t) u_c(x)$. The new POD decomposition for the variable u is then:

$$u(x,t) = \overline{u_h}(x) + \gamma(t)\, u_c(x) + \sum_{k=1}^{q} a_k(t)\, \varphi_h^{(k)}(x) \tag{23}$$

The forcing term is not completely defined as the shape of the spatial control function u_c has not yet been given. Several choices are possible since the only constraint imposed by $u_f(x = L, t) = \gamma(t)$ is that $u_c(x = L) = 1$. A Dirac distribution $u_c(x) = \delta(x - L)$ satisfies the previous condition but is certainly not

optimal because of the discontinuity inherent to this function. A better choice consists in choosing the static solution of the problem for a unitary displacement imposed at the free end: $u_c(x) = x/L$.

The reduced-order model is easily obtained by introducing the new decomposition Eq. (23) into the continuous equation of the rod and by projecting it onto each POM:

$$\begin{aligned} \frac{d^2 a_j}{dt^2} &= c^2 \sum_{k=1}^{q} \left\langle \frac{d^2 \varphi^{(k)}}{dx^2}, \varphi_h^{(j)} \right\rangle a_k + c^2 \left\langle \frac{d^2 \overline{u_h}}{dx^2}, \varphi_h^{(j)} \right\rangle \\ &\quad + c^2 \, \gamma(t) \left\langle \frac{d^2 u_c}{dx^2}, \varphi_h^{(j)} \right\rangle - \frac{d^2 \gamma(t)}{dt^2} \left\langle u_c, \varphi_h^{(j)} \right\rangle \end{aligned} \tag{24}$$

The form $\ddot{\mathbf{a}} = \widetilde{\boldsymbol{\mathcal{L}}}\,\mathbf{a} + \widetilde{\boldsymbol{\mathcal{K}}}$ of the reduced-order model is preserved but the matrix $\widetilde{\boldsymbol{\mathcal{L}}}$ and the vector $\widetilde{\boldsymbol{\mathcal{K}}}$ are now defined by:

$$\begin{aligned} \widetilde{\mathcal{L}}_{ij} &= c^2 \sum_{j=1}^{q} \left\langle \frac{d^2 \varphi^{(j)}}{dx^2}, \varphi_h^{(i)} \right\rangle \\ \widetilde{\mathcal{K}}_i &= c^2 \left\langle \frac{d^2 \overline{u_h}}{dx^2}, \varphi_h^{(i)} \right\rangle + c^2 \, \gamma(t) \left\langle \frac{d^2 u_c}{dx^2}, \varphi_h^{(i)} \right\rangle - \frac{d^2 \gamma(t)}{dt^2} \left\langle u_c, \varphi_h^{(i)} \right\rangle \end{aligned} \tag{25}$$

The three formulations given by Eqs. (19), (22) and (25) are clearly different. The Penalty Method (PM) is very easy to implement because the matrix and vector of the reduced-order model are the same as those obtained for the free response; they are only modified by the addition of a penalty matrix (or vector) which is easily computed once the POMs are known. The main drawback of the method is that the boundary condition is only approximated and not exactly satisfied. Indeed, the greater the penalty factor, the more exact the boundary condition but the more ill-conditioned the matrices. The Lagrange Multiplier Method (LMM) leads to the introduction of a new variable in the system which changes the form of the reduced-order model: indeed, the matrix $\widetilde{\boldsymbol{\mathcal{I}}}$ in the left member is singular and prevents finding again the same form common to the other formulations. Finally the CFM requires more modifications since the snapshots have to be first homogenized before computing the POMs. Another assumption is that the forcing term can be decomposed as the product of a spatial and a temporal function. The reduced-order model derived with the new decomposition keeps the same usual form but involves time derivatives of the boundary condition time modulation $\gamma(t)$.

3.4 Hybrid POD evaluation for the response to a prescribed displacement

The time integration of the reduced-order model is performed either by the ODEPACK solver or with a Newmark algorithm. This algorithm is especially adapted for the LMM where the differential equation cannot be written under the generic form $\dot{\mathbf{a}} = f(\mathbf{a}, t)$ which is solved by the ODEPACK. The efficiency of each formulation is evaluated by means of the error ε_∞ based on a reference solution $\mathbf{U}_r$ computed with a Finite Elements simulation and defined by:

$$\varepsilon_\infty = \frac{\|\mathbf{U} - \mathbf{U}_r\|_\infty}{\|\mathbf{U}_r\|_\infty} \tag{26}$$

The hybrid POD reduced-order model is used to reconstruct the response of the rod with a displacement imposed at the free end. The POMs are thus evaluated from a discrete set of snapshots which have been computed by a Finite Elements simulation for the forced response. The POMs for the PM and LMM, which are represented on Fig. 1 with the black filled circles, are identical. If the Control Function Method (CFM) is adopted, the snapshots have to be homogenized before computing the POMs. The shape of the POMs then depends on the control function used for the homogenization: if a Dirac function $u_c(x) = \delta(x - L)$ is used, the modes are similar to those of the PM or LMM except for the last point $x = L$ where the value is zero. On

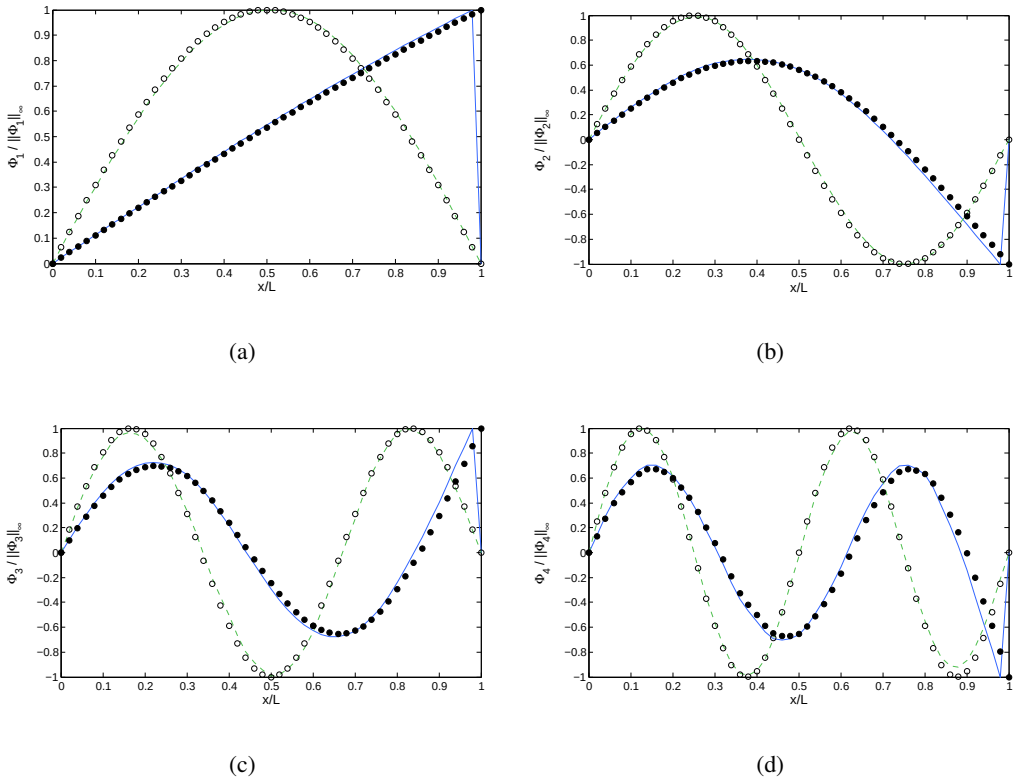

Figure 1: Comparison of the first four POMs for the forced response. The empty black circles (○) represent the eigenmodes of the rod clamped at both ends whereas the black filled circles (●) indicates the POMs of the forced response when the PM or LMM are used to impose the displacement. The curves (——) and resp. (— —) represent the shape of the POMs when the CFM is adopted and the control function is $u_c(x) = \delta(x - L)$ or resp. $u_c(x) = x/L$.

the contrary, with the static solution $u_c(x) = x/L$, the modes differ significantly from the previous ones: in this case, homogeneous boundary conditions are satisfied by the POMs at both ends of the rod but the shape does not exhibit any discontinuity. The POMs then coincide with the eigenmodes of a rod which would be clamped at both ends; these eigenmodes are represented with empty black circles on Fig. 1.

We then compare the efficiency of the three techniques (PM, LMM and CFM) to take into account a displacement $\gamma(t) = U_e \sin(2\pi f_e t)$ imposed at the free end. Figure 2 presents the response of the reduced-order model based on the CFM with $u_c(x) = x/L$ for three couples of parameters (f_e, U_e). The responses computed with the other methods (PM, LMM and CFM with $u_c(x) = \delta x - L$) are not shown since they are not distinguishable. For each response, the POMs have been computed from snapshots stemming from the resolution of the problem with the excitation parameters $(f_e, U_e) = (150, 0.01)$. This POD basis is then used to calculate the response for the three couples of parameters $(f_e, U_e) = (150, 0.01)$, $(f_e, U_e) = (200, 0.05)$ and $(f_e, U_e) = (325, 0.2)$ by introducing the desired imposed displacement $\gamma(t)$ characterized by each couple of parameters (f_e, U_e) in Eq. (25). In each case, the response coincide exactly with the reference solution which has been computed with a Finite Elements simulation.

To highlight the differences between the PM, LMM and CFM, the values of the infinite error ε_∞ are plotted on the figure 3.a. Except for the PM, the error grows as the parameters go away from those used to evaluate the POMs. This is the main limitation of the POD method: since the POD basis is constructed from snapshots, the basis vectors depend on the excitation and the reduced-order model becomes less efficient as the parameters for which the response has to be computed take away from those characterizing the excitation with which the snapshots, and consequently the POMs, have been obtained. Nevertheless, the errors remain

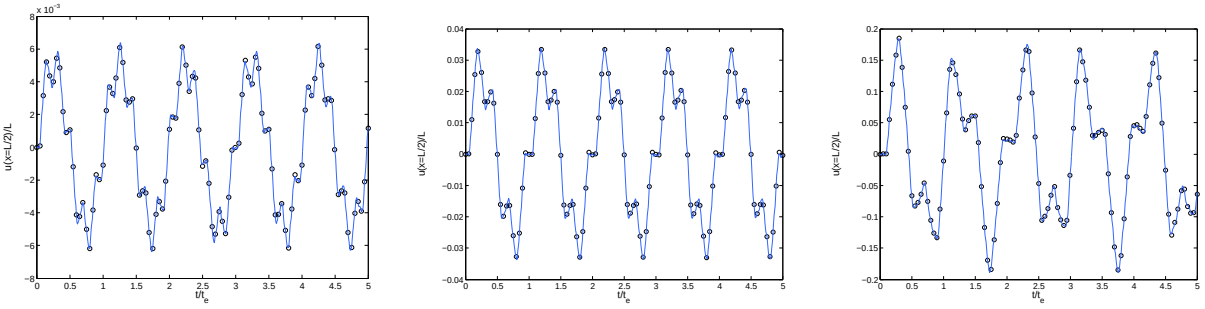

(a) (b) (c)

Figure 2: Comparison between the POD responses for the forced response computed for three different couples of excitation parameters (——) and the reference solution (○) : (a) $(f_e, U_e) = (150, 0.01)$, (b) $(f_e, U_e) = (200, 0.05)$, (c) $(f_e, U_e) = (325, 0.2)$.

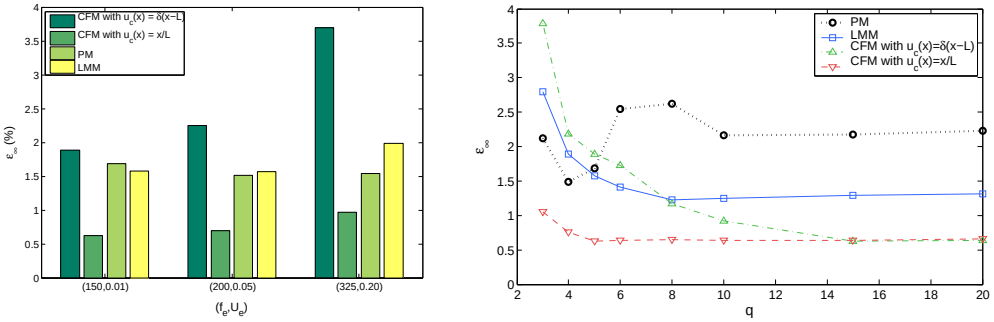

(a) (b)

Figure 3: Comparison of the infinite error ε_∞ produced by the different methods used to impose the displacement: (a) for different couples of excitation parameters (f_e, U_e), and (b) when the number of POMs used in the reduced-order model is increased.

small for this simple system and the responses obtained with the different formulations are in very good agreement with the reference solutions. The best method for this example seems to be the CFM when the POMs have been homogenized with the static solution of the system $u_c(x) = x/L$. However, the influence of the control function is crucial and it can be seen that the choice of the Dirac function for u_c leads to the greatest error.

Figure 3.b represents for each method the convergence of the infinite reconstruction error ε_∞ when the number q of POMs contained in the POD basis is increased. The PM has in fact the greatest asymptotic error and does not converge very well. The best method is actually the CFM with the static solution, but when the number of POMs is increased, we notice that the use of the Dirac function becomes a reliable choice, better than the PM or even the LMM. This is an interesting result since the use of a Dirac does not require the computation of a physical solution of the system like it is the case with the static solution, whose determination could become time-consuming when the number of dof at the boundary is great.

The CFM seems to be the most efficient method but the choice of the control function used for the homogenization is capital. Moreover, when a displacement u_L is imposed at the free end, it is necessary to know the acceleration $\ddot{u}_L$ associated to this displacement in order to evaluate the coefficients $\widetilde{\mathcal{K}}_i$ of the reduced-order

model defined in Eq. (25). It is trivial to determine the acceleration for a sinusoidal displacement like the one imposed here, but some difficulties can arise if other shapes are used (e.g. a sawtooth or crenel function which is not derivable). Sometimes, the displacement is also not explicitly known (e.g. the case of a coupled fluid-structure system) and determining the acceleration is not obvious. The PM and LMM avoid this drawback and have besides the advantage to be more flexible: the POD basis used in the reduced-order model can eventually come from snapshots corresponding to the free response, or the forced response with a force (instead of a displacement) imposed at the free end. This could also be done with the CFM but it requires the determination of the adequate time modulations $\gamma(t)$ in order to homogenize the snapshots.

4 Robustness of the hybrid POD method

In this section, the robustness of the hybrid POD formulation is investigated in the case of a non-linear response produced by a clamped-free rod excited by a force F whose application point is distant of $x_f < L$ from the clamped end. An obstacle is placed at the distance e from the free end (see Fig. 4). When the magnitude of the force is enough important, the free end section hits the obstacle; this generates vibro-impacts and therefore produces a reaction at this point. The reaction is non-linear and defined by $R(u_L) = -K_{obs}(u_L - e)$ if $u_L > e$ and $R(u_L) = 0$ if $u_L \leq e$. The excitation force is sinusoidal and characterized by $F(t) = F_e \sin(2\pi f_e t)$. According to the values of F_e and f_e, the free end hits or not the obstacle, whose stiffness has a great value ($K_{obs} = 10^{20}$) in order to model a rigid obstacle.

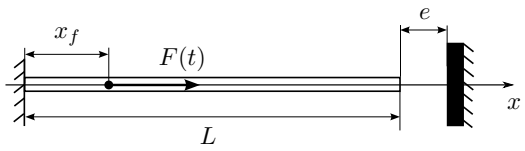

Figure 4: Clamped-free rod excited by the force F and subject to vibro-impacts due to the obstacle.

In this example, the POMs are significantly different from those of the free or forced response. Figure 5 gives the shape of the POMs obtained from a set of snapshots computed with or without the obstacle. In both cases, the excitation force F is characterized by $(f_e, F_e) = (175, 2.0\text{E}6)$. When the rod hits the obstacle, the non-linear reaction at the free end leads to a more complex response of the system than when there is no obstacle. In both cases (with or without the obstacle), the shape of the POMs is very different from the rod eigenmodes: the force F applied at $x_f = 0.1\,L$ deforms considerably the shape of the modes in the neighborhood of this point.

The response of the system for different couples of parameters (f_e, F_e) is then computed. Figure 6 shows the responses when the POMs used in the reduced-order model have been evaluated from snapshots with the obstacle. For the first (a) and last (c) cases, the magnitude of the imposed force F_e is great enough so that the free end hits the obstacle, whereas in the intermediate case (b) there is no contact between the free end and the obstacle. Although the POMs stem from snapshots with vibro-impacts, they are suitable to rebuild the responses either with or without contact. The hybrid POD formulation is considered to be robust since the reduced-order model can be used to rebuild diverse responses with POMs stemming from snapshots computed for a different type of excitation (with or without obstacle, or even POMs coming from the free response of the system).

Although Fig. 6 exhibits a somewhat good accuracy of the response, the errors produced become now significant, notably when vibro-impacts occur. The errors are plotted on Figure 7 for the three couples of parameters and according to the nature of the POMs used in the reduced-order model. When the free end hits the obstacle (first and last cases), the error is almost the same, whatever the nature of the POMs: despite slight differences appear according to the type of the POMs used, the error has the same order of magnitude. On the contrary, if no contact happens, the POMs computed from snapshots without the obstacle are clearly

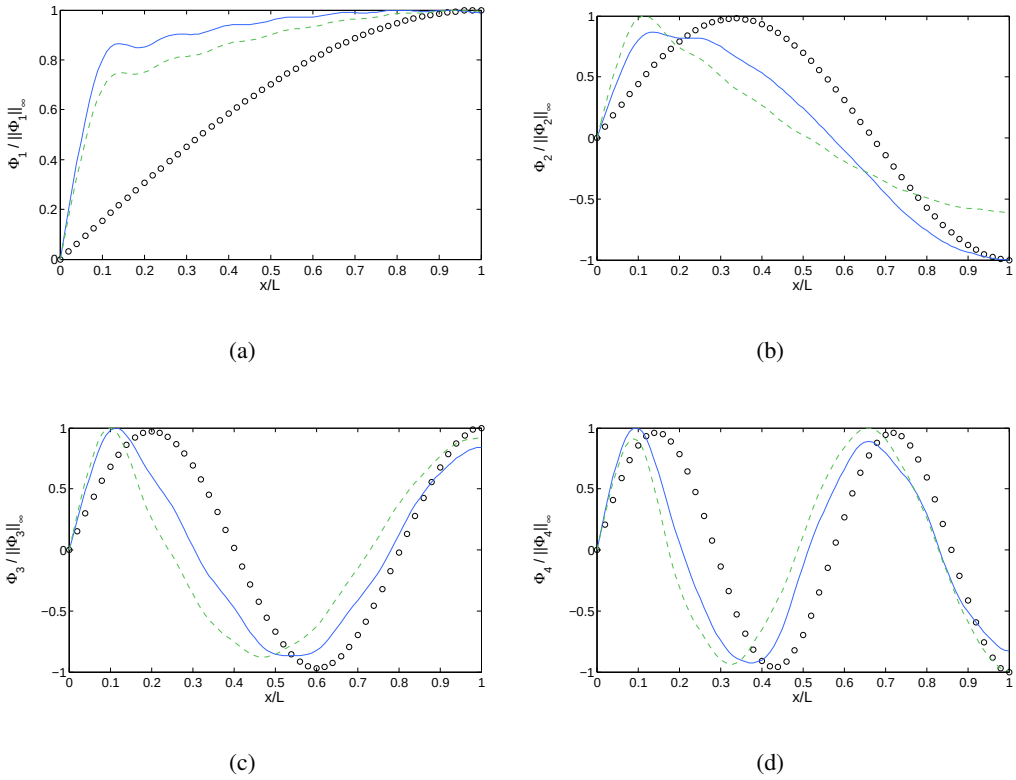

Figure 5: Panels (a)-(d) show the first four POMs of the rod subject to vibro-impacts and computed from snapshots with the obstacle (——) or without it (– –). The black circles (○) represent the rod eigenmodes.

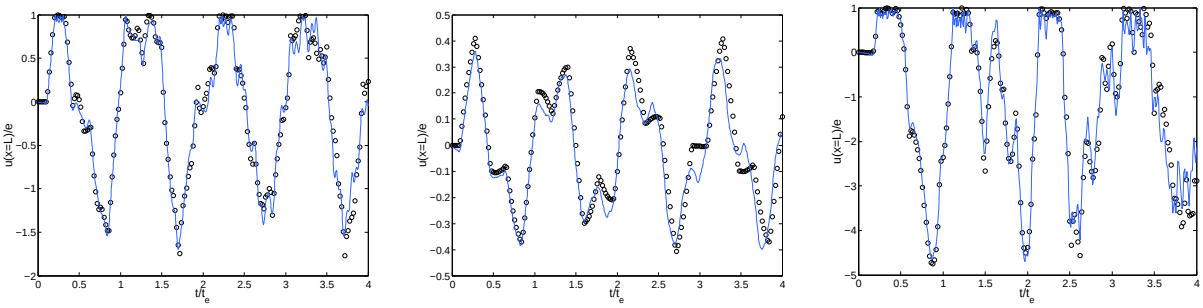

Figure 6: Comparison between the responses for the rod subject to vibro-impacts computed for three different couples of excitation parameters (——) and the reference solution (○): (a) $(f_e, F_e) = (175, 2.0\text{E}6)$, (b) $(f_e, F_e) = (150, 0.5\text{E}6)$, (c) $(f_e, F_e) = (300, 5.0\text{E}6)$.

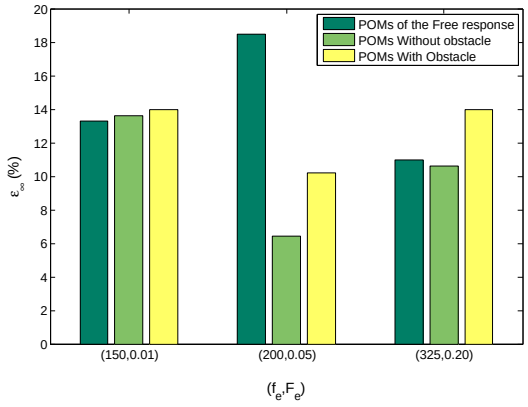

Figure 7: Comparison of the infinite reconstruction error ε_∞ for different couples of parameters according to the nature of the POMs used.

more efficient than the others. The POMs of the free motion give the greatest error when no contact happens, however the results are in good agreement in other cases.

To conclude, the POD method provides a rather robust mean to build a reduced-order model: when the response is computed with POMs which have been evaluated for the same type of excitation, the accuracy is in general very good. However, the use of POMs stemming from a different type of excitation is a more delicate issue. The POMs of the free response could be employed easily to rebuild responses for other types of excitations (e.g. response with structural damping or with a non-linear reaction induced by an obstacle, response to an imposed displacement with the PM or LMM) but this is somewhat obvious since in this particular case the POMs are close to the eigenmodes of the system. However, if we want to rebuild the free response to an initial condition, the use of POMs obtained from snapshots with a displacement or a force imposed is not appropriate since the POMs do not satisfy the suitable boundary conditions and the reduced-order model has to be adapted.

5 Conclusion

In this paper the hybrid POD formulation has been evaluated and compared for the response to a prescribed displacement. Several methods have been compared and advantages and drawbacks have been highlighted. Except the PM which has a surprising convergence behavior when the number of POMs in the projection basis is increased, the other methods (LMM and CFM) behave well and the asymptotic error remains small. The CFM is the most accurate but has several drawbacks, particularly the sensitivity to the control function or the need for the time derivative of the excitation function. However, once a good control function has been determined, the method is robust and converge very quickly as the number of POMs is increased. Finally, the results of the last paragraph show that hybrid POD is a rather robust method: the POMs obtained from snapshots computed for a simple excitation (e.g. the response to an initial condition) seem to provide a good basis to rebuild responses of diverse types, even for responses which are far from the one used to compute the POMs.

This study that fits into the framework of the construction of reduced-order models for coupled fluid-structure systems gives prominence to interesting results concerning the potential of the hybrid POD to build an efficient reduced-order model and is therefore encouraging us to use this formulation for future applications, the next one being the reduction of the fluid.

References

[1] M. Loève, *Probability Theory*, D. Van Nostrand, 1960.

[2] S. Volkwein, *Proper Orthogonal Decomposition and Singular Value Decomposition*, SFB-Preprint No. 153 (1999). URL `www.uni-graz.at/imawww/volkwein/svd.ps`

[3] Y. Liang, H. Lee, S. Lim, W. Lin, K. Lee, C. Wu, *Proper orthogonal decomposition and its applications - Part I: Theory*, Journal of Sound and Vibration, Vol. 252, No. 3 (2002), pp. 527–544.

[4] J. Lumley, *The Structures of Inhomogeneous Turbulent Flow*, edited by A.M. Yaglom and V.I. Tatarski, Nauka, Moscow Edition, Atmospheric Turbulence and Radio Wave Propagation, 1967, pp. 166–178.

[5] D. Lucia, P. Beran, W. Silva, *Reduced-order modeling : New approaches for computational physics*, Progress in Aerospace Science, Vol. 40 (2004), pp. 51–117.

[6] E. Dowell, K. Hall, J. Thomas, R. Florea, B. Epureanu, J. Hegg, *Reduced order models in unsteady aerodynamics*, AIAA Paper 1999-1261.

[7] G. Kerschen, J.-C. Golinval, A. Vakakis, L. Bergman, *The method of proper orthogonal decomposition for dynamical characterization and order reduction of mechanical systems : An overview*, Nonlinear Dynamics, Vol. 41 (2005), pp. 147–169.

[8] B. Feeny, R. Kappagantu, *On the physical interpretation of proper orthogonal modes in vibrations*, Journal of Sound and Vibration, Vol. 211, No.4 (1998), pp. 607–616.

[9] G. Kerschen, J.-C. Golinval, *Physical interpretation of the proper orthogonal modes using the singular value decomposition*, Journal of Sound and Vibration, Vol. 249, No. 5 (2002), pp. 849–865.

[10] M. Amabili, A. Sarkar, M. Païdoussis, *Chaotic vibrations of circular cylindrical shells : Galerkin versus reduced-order models via the proper orthogonal decomposition method*, Journal of Sound and Vibration, Vol. 290, No. 3-5 (2006), pp. 736–762.

[11] S. Bellizzi, R. Sampaio, *POMs analysis of randomly vibrating systems obtained from Karhunen-Loève expansion*, Journal of Sound and Vibration, Vol. 297, No. 3-5 (2006), pp. 774–793.

[12] M. Azeez, A. Vakakis, *Proper orthogonal decomposition (POD) of a class of vibroimpact oscillations*, Journal of Sound and Vibration, Vol. 240, No. 5 (2001), pp. 859–889.

[13] R. Sampaio, C. Soize, *Remarks on the efficiency of POD for model reduction in non-linear dynamics of continuous elastic systems*, International Journal for Numerical Methods in Engineering, Vol. 72 (2007), pp. 22–45.

[14] A. Placzek, D.-M. Tran, R. Ohayon, *Hybrid proper orthogonal decomposition formulation for linear structural dynamics*, Journal of Sound and Vibration, DOI:10.1016/j.jsv.2008.05.015.

[15] K. Tang, W. Graham, J. Peraire, *Active flow control using a reduced order model and optimum control*, (1996). URL `citeseer.ist.psu.edu/tang96active.html`

[16] P. Holmes, J. Lumley, G. Berkooz, *Turbulence, Coherent Structures, Dynamical Systems and Symmetry*, Cambridge University Press, 1996.

[17] L. Sirovich, *Turbulence and the dynamics of coherent structures, Parts I-III*, Quarterly of Applied Mathematics, Vol. XLV (1987), pp.561–590.

[18] Y. Tamura, S. Suganuma, H. Kikuchi, K. Hibi, *Proper orthogonal decomposition of random wind pressure field*, Journal of Fluids and Structures, Vol. 13, No. 7-8 (1999), pp. 1069–1095.

Office National d'Études et de Recherches Aérospatiales
BP 72 - 29 avenue de la Division Leclerc
92322 CHATILLON CEDEX
Tél. : +33 1 46 73 40 40 - Fax : +33 1 46 73 41 41
http://www.onera.fr